Chemical Science

ROYAL SOCIETY OF CHEMISTRY

PERSPECTIVE

View Article Online
View Journal | View Issue

Cite this: *Chem. Sci.*, 2021, **12**, 10972

All publication charges for this article have been paid for by the Royal Society of Chemistry

Received 12th May 2021
Accepted 7th July 2021

DOI: 10.1039/d1sc02614c

rsc.li/chemical-science

Sulfur stereogenic centers in transition-metal-catalyzed asymmetric C–H functionalization: generation and utilization

Wentan Liu, Jie Ke and Chuan He *

Transition-metal-catalyzed enantioselective C–H functionalization has emerged as a powerful tool for the synthesis of enantioenriched compounds in chemical and pharmaceutical industries. Sulfur-based functionalities are ubiquitous in many of the biologically active compounds, medicinal agents, functional materials, chiral auxiliaries and ligands. This perspective highlights recent advances in sulfur functional group enabled transition-metal-catalyzed enantioselective C–H functionalization for the construction of sulfur stereogenic centers, as well as the utilization of chiral sulfoxides to realize stereoselective C–H functionalization.

1. Introduction

Transition-metal-catalyzed C–H functionalization has emerged as a powerful tool for the construction of C–C and C–heteroatom bonds owing to its high step and atom economy.[1–7] By viewing the C–H bond as "ubiquitous functionality", synthetic chemists open a new chapter in organic synthesis, which has revolutionised the rules for assembling molecules. In particular, new catalytic transformations based on the enantioselective functionalization of C–H bonds have attracted considerable attention,[8–12] given the paramount importance of chirality in organic molecules and growing demand for enantiopure compounds in chemical and pharmaceutical industries. Although asymmetric C–H functionalization is still in its infancy, the recently developed chiral directing groups (cDGs) and chiral ligands have armed this promising methodology to streamline the synthesis of various chiral molecules in an atom- and step-economical manner.

Sulfur-based functionalities are ubiquitous in many of the biologically active compounds, medicinal agents, and functional materials. Biomolecules containing sulfur stereocenters play an important role in the chemical reactions of general metabolism.[13] Owing to their significant bioactivity, an increasing number of marketed drugs and bioactive compounds contain sulfoxides and sulfoximines in enantiopure form.[14–18] Moreover, organosulfur compounds are commonly utilized as starting materials, reagents, or intermediates in synthetic organic chemistry,[19–22] in which chiral sulfoxides are particularly useful in asymmetric catalysis as versatile chiral auxiliaries or ligands due to their high optical stability (Scheme 1).[23–27] Traditional strategies toward enantioenriched sulfoxides mainly rely on resolution techniques and diastereoselective transformations, in which the need for stoichiometric amounts of chiral-pool reagents has made their synthetic application cumbersome.[28] So far, the most popular routes for the access of enantioenriched sulfoxides have been metal-catalyzed and biocatalytic asymmetric sulfide oxidation processes. However, the requirement for discrimination between the substituents of sulfides usually limits their utility.[29]

Given the importance of asymmetric C–H functionalization technology in modern synthetic chemistry, as well as the abundance of chiral organosulfur compounds in biologically active compounds, pharmaceuticals and materials, the generation and utilization of sulfur stereogenic centers in transition-metal-catalyzed asymmetric C–H functionalization is undoubtably highly attractive. This Perspective is aimed to comprehensively highlight recent advances in sulfur functional group directed transition-metal-catalyzed enantioselective C–H functionalization for the construction of sulfur stereogenic centers,

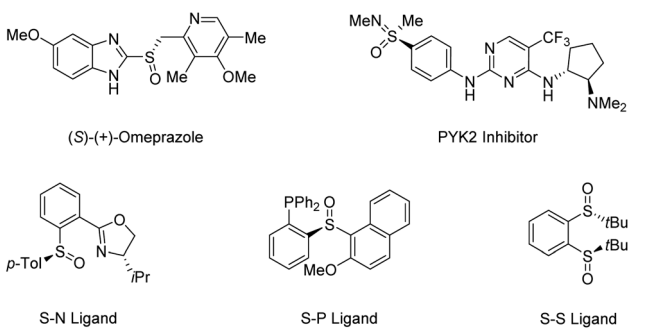

Scheme 1 Representative bioactive molecules and ligands containing sulfur stereogenic centers.

Shenzhen Grubbs Institute, Department of Chemistry, Guangdong Provincial Key Laboratory of Catalysis, Southern University of Science and Technology, Shenzhen, Guangdong 518055, China. E-mail: hec@sustech.edu.cn

as well as the utilization of chiral sulfoxides to steer stereoselective C–H functionalization. We hope to shed light on new perspectives, and inspire the use, the completion, and the improvement of this emerging methodology, which could be attractive to practitioners of medicinal chemistry and materials science.

2. Generation of sulfur stereocenters through enantioselective C–H functionalization

In recent years, sulfoxides and sulfoximines have found a unique place in C–H functionalization owing to their various modes of reactivity. A number of sulfoxide and sulfoximine directed C–H functionalization reactions have successfully been demonstrated.[30–32] Importantly, an additional advantage of these scaffolds is their potentially stereogenic character, and thus enantioselective C–H functionalization reactions could be explored for the facile generation of sulfur stereogenic centers.

2.1 Sulfoxide-directed enantioselective C–H functionalization

In 2018, Wang and co-workers reported a Pd(II)-catalyzed enantioselective C–H olefination with non-chiral and racemic diaryl sulfoxides *via* desymmetrization and parallel kinetic resolution (PKR) (Scheme 2).[33] The optimization of a range of different monoprotected amino acids revealed that Ac-Leu-OH was the best ligand for this transformation. It is worth mentioning that pre-stirring of the chiral amino acid ligand

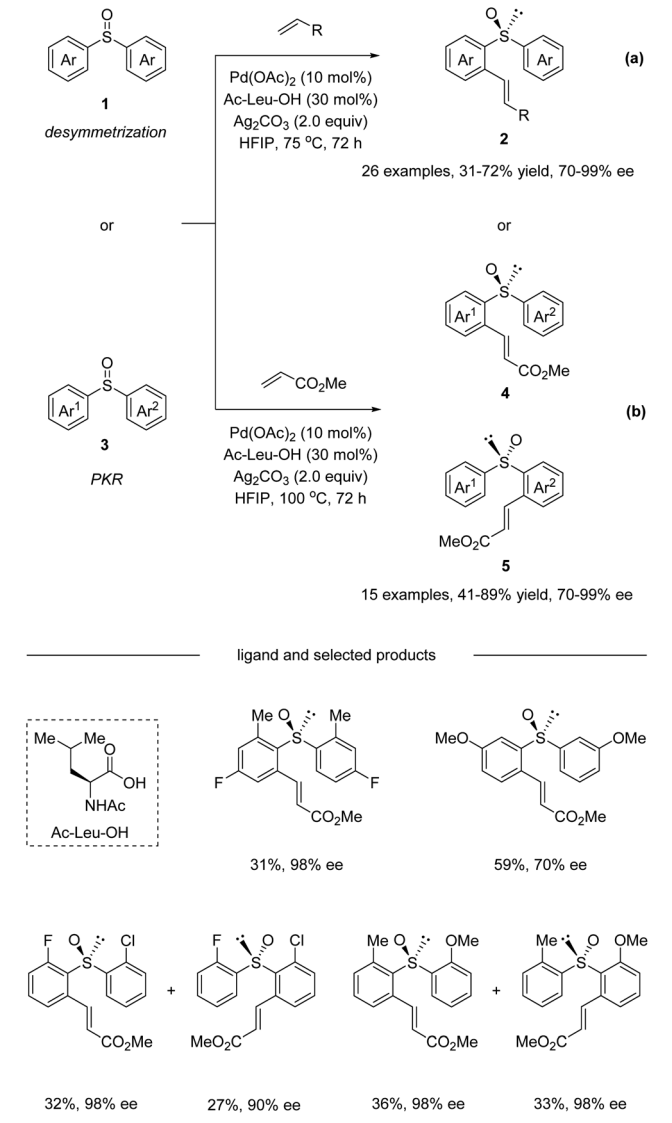

Scheme 2 Pd(II)-catalyzed enantioselective C–H olefination of diaryl sulfoxides. (a) Desymmetrization pathway. (b) Parallel kinetic resolution pathway.

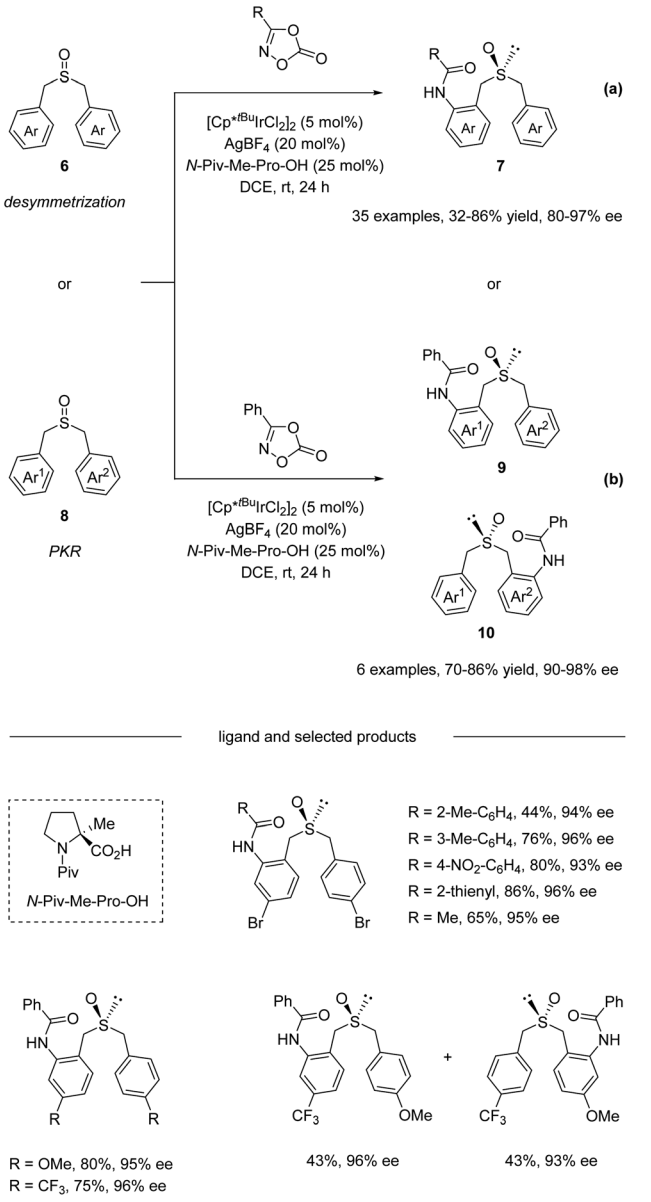

Scheme 3 Dual-ligand-enabled Ir(III)-catalyzed enantioselective C–H amidation of dibenzyl sulfoxides. (a) Desymmetrization pathway. (b) Parallel kinetic resolution pathway.

with $Pd(OAc)_2$ is essential, because the coordination ability of sulfoxide could influence their complexation. Under the optimized conditions, the desymmetrization of symmetric diaryl sulfoxides **1** afforded *ortho* substituted olefination products **2** in moderate yields with good enantioselectivities (Scheme 2a). Substrates bearing electron-neutral, electron-donating, and weakly electron-withdrawing substituents or *para*, *meta*, and *ortho* substituents were all tolerated. Aside from methyl acrylate, diethyl vinyl phosphonate and pentafluoro-styrene were also competent reaction partners delivering the corresponding products with good ee. Additionally, non-symmetric diaryl sulfoxides **3** were converted in a parallel kinetic resolution pathway (Scheme 2b) to give two products from the racemic starting materials. Diaryl sulfoxides reacted to give products **4** and **5** in excellent enantioselectivity *via* stereo-divergent olefination.

In 2020, He and co-workers reported an Ir(III)-catalyzed asymmetric C–H amidation of pro-chiral and racemic dibenzyl sulfoxides (Scheme 3).[34] A survey of a range of different chiral carboxylic acid ligands and achiral Cp ligands revealed that *N*-Piv-Me-Pro-OH and Cp^{*tBu} were the optimal ligands for this transformation, providing an efficient and straightforward way to construct sulfur chiral centers. A variety of dibenzyl sulfoxides and dioxazolones were compatible with this process, giving access to a variety of highly functionalized sulfoxide compounds with synthetically attractive amide substitution groups in good yields with excellent enantioselectivities *via* desymmetrization (Scheme 3a) and parallel kinetic resolution (PKR, Scheme 3b). Moreover, the flexible derivatization of the amidated sulfoxide was elaborated, providing various types of chiral sulfoxide scaffolds that could be potentially useful in asymmetric catalysis as chiral bidentate and tridentate ligands.

The catalytic cycle starts with the coordination of active species **11** with dibenzyl sulfoxide, giving intermediate **12.** Then enantioselective C–H bond activation occurs as the rate-determining step (RDS) with a 6.4 KIE value *via* concerted metalation/deprotonation (CMD) assisted by chiral carboxylic

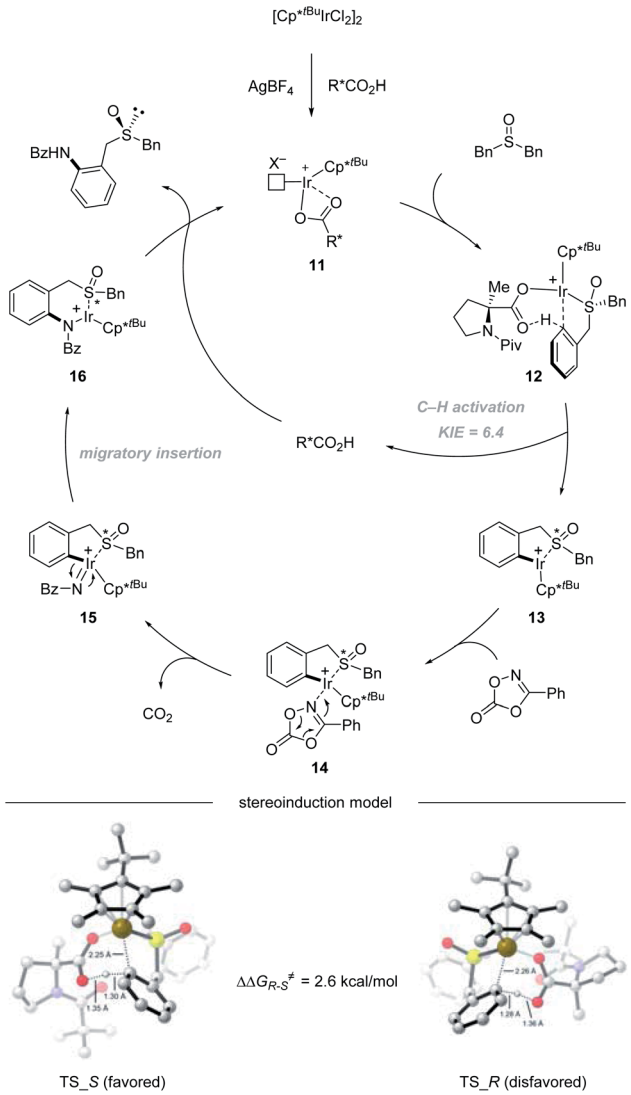

Scheme 4 Mechanism of Ir(III)-catalyzed enantioselective C–H amidation of dibenzyl sulfoxides.

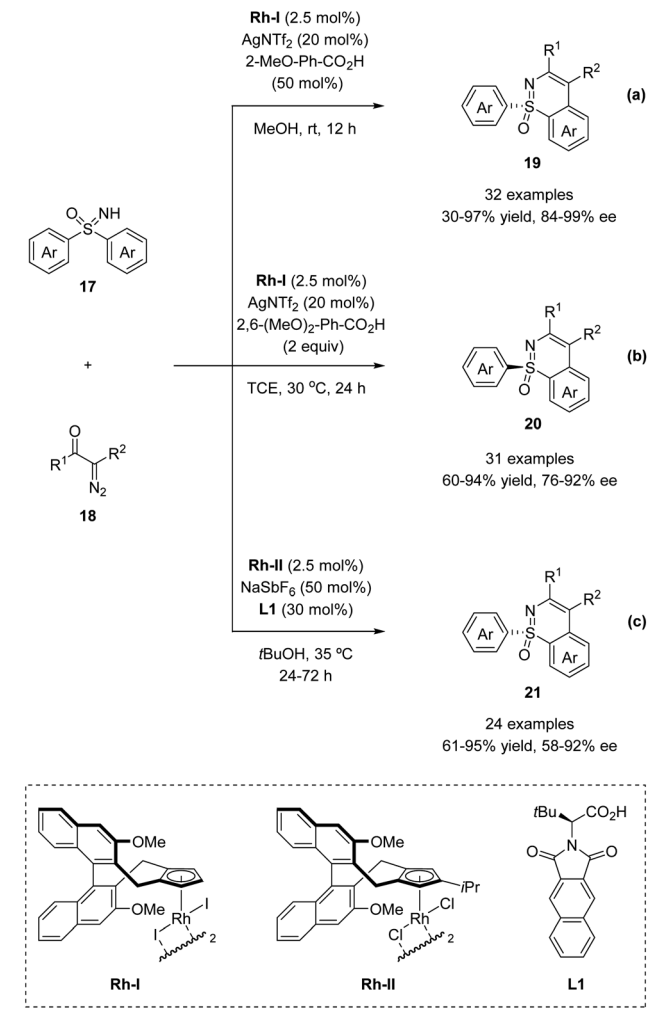

Scheme 5 $Cp^{x}Rh(III)$-catalyzed enantioselective annulative C–H functionalization of diaryl sulfoximines. (a and b) Li's work toward (*R*) and (*S*)-products by altering carboxylic acid and solvent. (c) Cramer's work toward (*R*)-products.

acid, providing (*S*)-iridacycle **13**. Preliminary DFT calculations reveal that **TS_*S*** is 2.6 kcal mol^{-1} lower in energy than **TS_*R***. The synergistic use of the Cp*$^{t\mathrm{Bu}}$ ligand with the (Piv)-protected methyl substituted tertiary proline ligand creates a compact chiral transition state, which allows the perfect discrimination of the diastereotopic benzyl groups. Then, the coordination of dioxazolone with intermediate **13** generates intermediate **14**, which can subsequently undergo CO_2 extrusion (intermediate **14** to **15**) and migratory insertion furnishes the desired amide bond (intermediate **15** to **16**). Finally, protonolysis produces the amide product and regenerates **11**, closing the catalytic cycle (Scheme 4).

2.2 Sulfoximine-directed enantioselective C–H functionalization

In 2018, the Li group and Cramer group independently reported the desymmetrization of diaryl sulfoximines under Rh(III)-catalyzed enantioselective annulative C–H functionalization with diazo compounds (Scheme 5).[35,36]

Li and co-workers applied the chiral Cp^{x}Rh(III) catalyst **Rh-I** in combination with differently substituted achiral benzoic acid derivatives, achieving an enantiodivergent desymmetrization of sulfoximines **17**. The use of **Rh-I** with 2-methoxybenzoic acid gave benzothiazines (*R*)-**19** in high yields with good enantioselectivities (Scheme 5a). A broad scope of sulfoximines bearing various electron-donating, electron-withdrawing, and halogen substituted groups were coupled with diazo reagents successfully (Scheme 6). Interestingly, an optimal inversion of

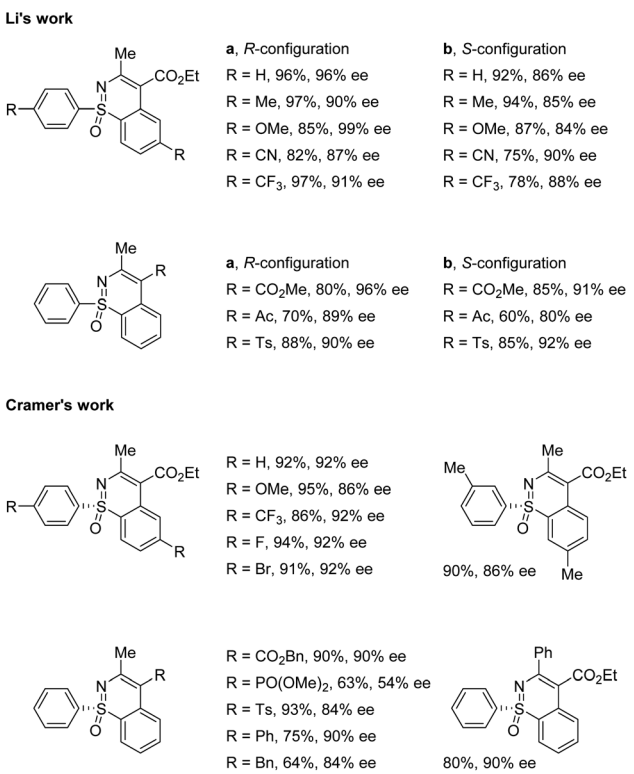

Scheme 6 Selected substrate scope.

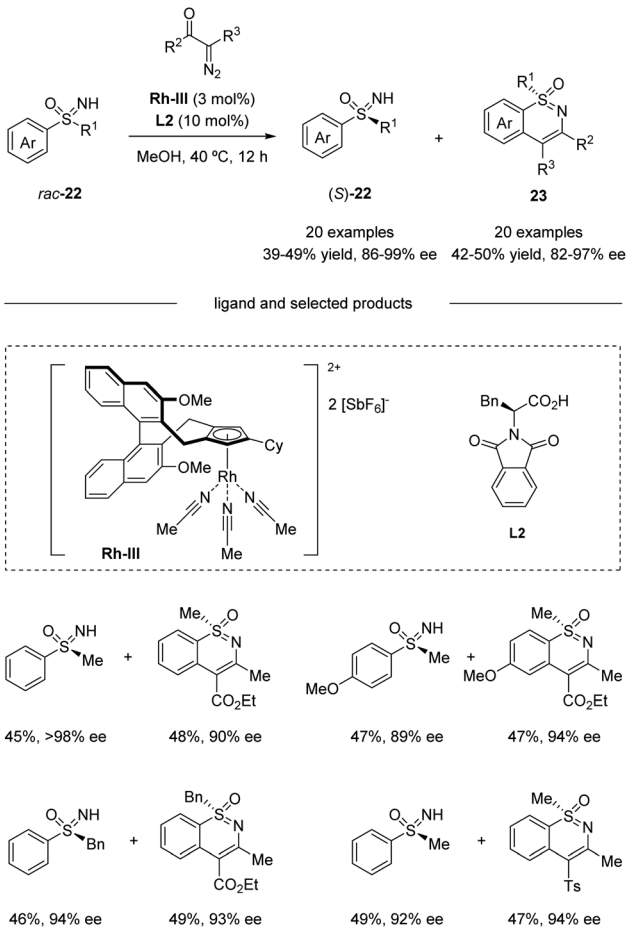

Scheme 7 Kinetic resolution of alkyl aryl sulfoximines *via* Cp^{x}Rh(III)-catalyzed annulative C–H functionalization.

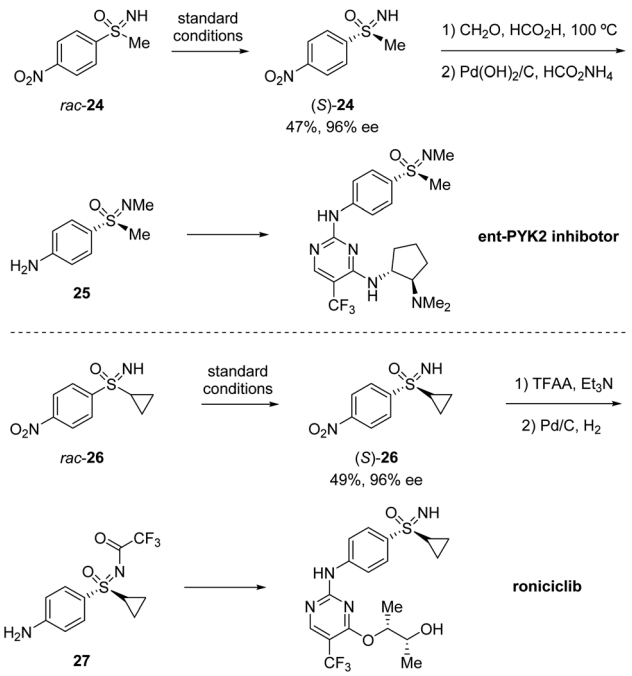

Scheme 8 Application of the kinetic resolution for bioactive compounds.

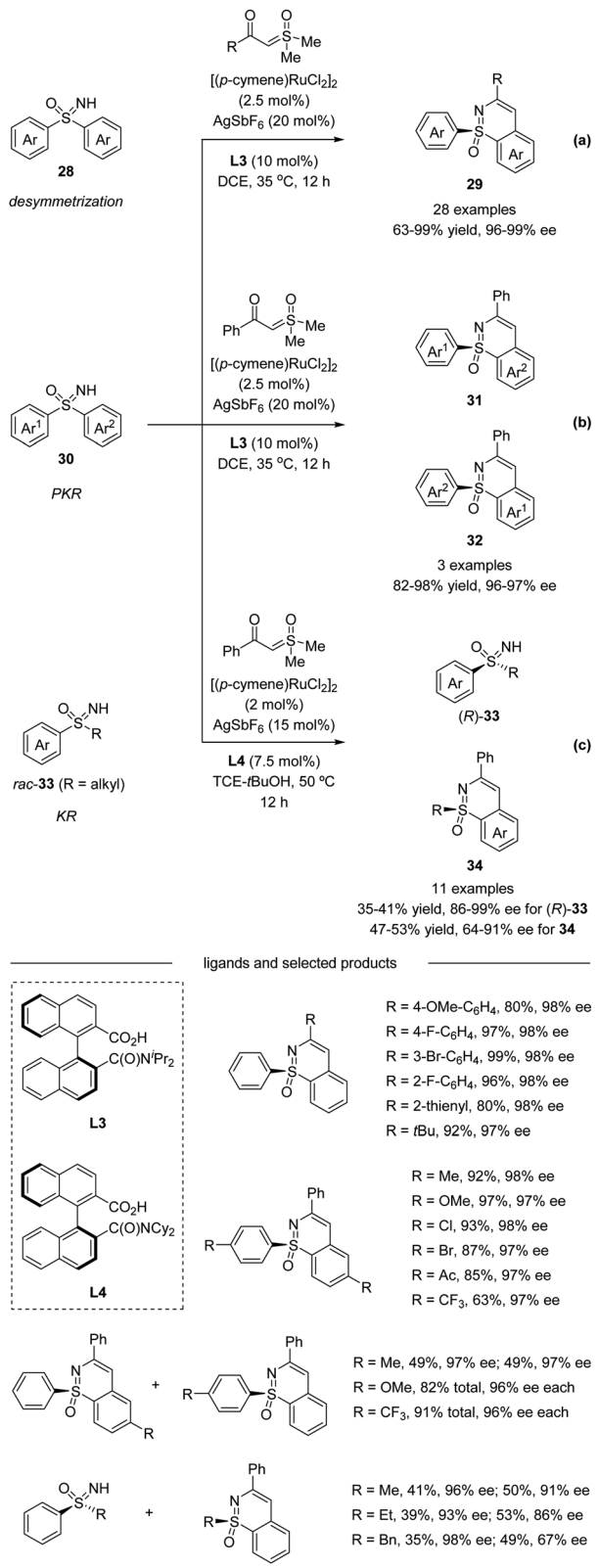

Scheme 9 Ru(II)-catalyzed enantioselective annulative C–H functionalization of diaryl sulfoximines and alkyl aryl sulfoximines. (a) Desymmetrization pathway. (b) Parallel kinetic resolution pathway. (c) Kinetic resolution pathway.

enantioselectivity was achieved when 2,6-dimethoxybenzoic acid was applied in the less polar solvent TCE (1,1,2,2-tetrachloroethane), and the opposite enantiomers (*S*)-**20** could be obtained with moderate to good enantioselectivities (Scheme 5b).

Meanwhile, Cramer and co-workers applied their trisubstituted chiral Cp^x ligand **Rh-II** in combination with chiral *tert*-leucine-derived ligand **L1**, also obtaining the annulative C–H functionalization products (*R*)-**21** in high yields with good enantioselectivities (Scheme 5c). A variety of diaryl sulfoximines with different substitution patterns and a series of diazo compounds proved to be capable reaction partners for this transformation (Scheme 6).

Based on their previous work, Cramer *et al.* further developed a kinetic resolution of alkyl aryl sulfoximines *via* cationic Cp^xRh(III)-catalyzed annulative C–H functionalization (Scheme 7).[37] By using chiral **Rh-III** and phenylalanine-derived ligand **L2**, they realized the conversion of racemic alkyl aryl substituted sulfoximines **22** to cyclic benzothiazines **23** and maintained enantioenriched starting materials (*S*)-**22** with high enantioselectivities. A variety of different aryl and alkyl substituted sulfoximines **22** and various diazo interceptors were well tolerated in the process. Additionally, the derivatization of the enantioenriched starting materials gave the precursors of bio-active molecules PYK2 inhibitor and roniciclib (Scheme 8).[38,39]

Very recently, Shi *et al.* described a Ru(II)-catalyzed enantioselective C–H activation/annulation of sulfoximines with α-carbonyl sulfoxonium ylides using C_1-symmetric binaphthyl

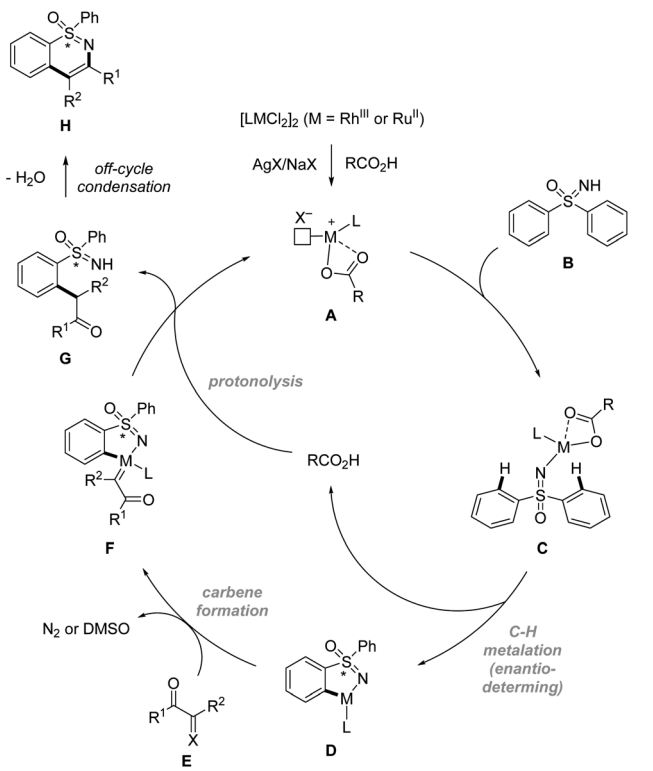

Scheme 10 Proposed mechanism of sulfoximine directed enantioselective C–H functionalization.

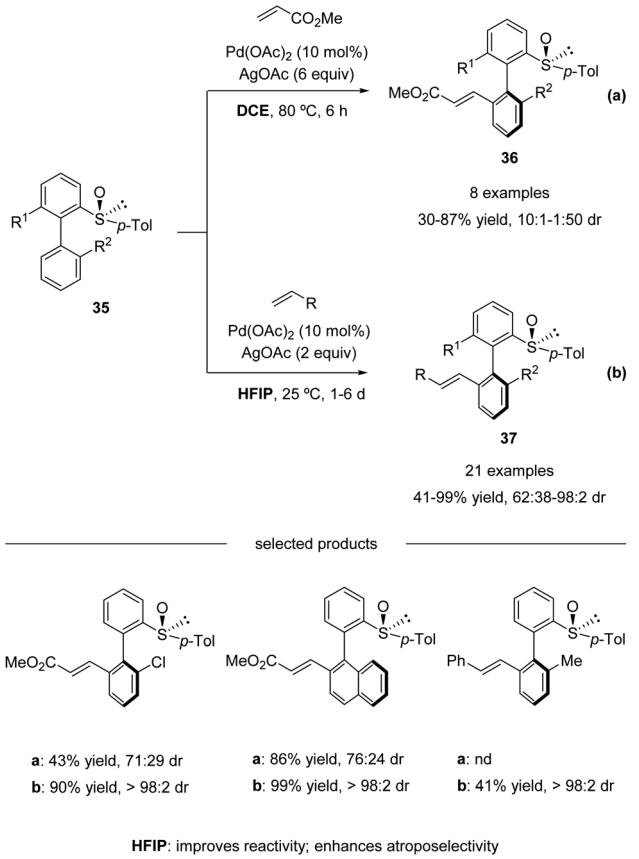

Scheme 11 Pd(II)-catalyzed sulfoxide-directed *atropo*-diastereoselective C–H olefination of biphenyls. (a) DCE as the solvent. (b) HFIP as the solvent.

monocarboxylic acids as chiral ligands *via* desymmetrization (Scheme 9a), parallel kinetic resolution (PKR, Scheme 9b), and kinetic resolution (KR, Scheme 9c).[40] A wide range of sulfoximines bearing various electron-donating groups and electron-withdrawing groups worked well with sulfoxonium ylides affording high yields with good to excellent enantioselectivities. α-Substituted benzoyl sulfoxonium ylides bearing electron-donating groups or halide substituents at the *para*, *meta*, and *ortho* positions of the aryl ring were all well-tolerated. α-Fatty acyl sulfoxonium ylides were also compatible with this transformation. Moreover, chiral sulfoximines obtained from kinetic resolution could be reduced stereospecifically to chiral sulfoxides. The inhibitors of human CYP24 hydroxylase could also be accessed from enantioenriched sulfoximines.

In terms of mechanism, the above sulfoximine directed enantioselective C–H functionalization reactions are proposed to begin with the formation of catalytically reactive species A. Then sulfoximine directed enantioselective C–H activation *via* concerted metalation/deprotonation (CMD) pathways gives metallacycle D. After that, carbene formation followed by migratory insertion of the M–aryl bond into the resulting carbene species leads to C–C bond formation. Finally, protonolysis and off-cycle condensation afford the annulated product H (Scheme 10).

3. Utilization of sulfur stereocenters in asymmetric C–H functionalization

Sulfoxides are classical functional groups for directing the stoichiometric metalation[41–45] and functionalization of C–H bonds. In recent years, a renaissance period in the application of sulfoxides arises from their versatility in directing C–H functionalization due to their unique reactivity. Furthermore, chiral sulfoxides have been considered as ideal ligand candidates for transition-metal-catalyzed asymmetric reactions due to their ready advantages of easy synthesis, stability, and special stereogenic control.

3.1 Chiral sulfoxide-directed diastereoselective C–H functionalization

In 2013, Colobert and co-workers reported the first *atropo*-diastereoselective method for the synthesis of axially chiral biaryl scaffolds *via* C–H olefination using a chiral sulfoxide both as the directing group enabling the regioselective activation of a C–H bond and as the chiral auxiliary generating an asymmetric environment in the coordination sphere of the metal complex (Scheme 11a).[46]

Electron-deficient acrylates serve as efficient coupling partners, giving access to *ortho*-alkenylated products **36** in moderate to good yields and *atropo*-diastereoselectivities (Scheme 11a). However, a relatively high reaction temperature (80 °C), a large excess of silver-based oxidant (6 equiv. of AgOAc), and activated

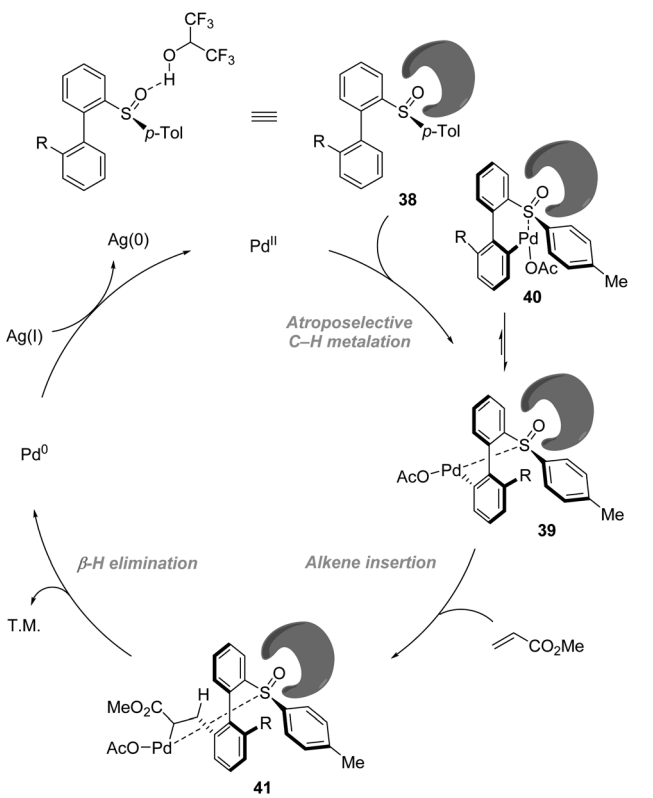

Scheme 12 Role of HFIP in the improvement of reactivity and enhancement of *atropo*-diastereoselectivity.

olefin coupling partners were needed in this process. To address these issues, they revisited their pioneering work and found that the use of 1,1,1,3,3,3-hexafluoroisopropanol (HFIP) as the solvent enhanced the reactivity significantly. The amount of oxidant could be reduced, and the reactions could run at ambient temperature, albeit with a long reaction time. Both acrylates and styrenes worked properly in the solvent of HFIP. Under the update conditions, high yields with excellent *atropo*-diastereoselectivities were obtained (Scheme 11b).[47]

On the basis of NMR and IR studies, Colobert and co-workers showed that the hydrogen-bond donor solvent HFIP might coordinate to the oxygen of the sulfoxide group, affecting the electronics of the directing sulfoxide group and enhancing the rate determining C–H activation step (KIE = 2.2 in DCE *vs.* KIE = 5.9 in HFIP). This sulfoxide–HFIP interaction plays a key role in achieving high *atropo*-diastereoselectivity, which may be ascribed to the increased effective size of the sulfoxide directing group when coordinated to HFIP. The catalytic cycle starts with the coordination between $Pd(OAc)_2$ and HFIP coordinated biarylsulfoxide substrate **38**. Then irreversible, rate-determining C–H bond cleavage occurs, affording the favourable atropisomeric palladacyclic intermediate **39** with a decreased steric hindrance. Then, the insertion of the olefin coupling partner into the C–Pd bond, followed by β-H elimination, delivers an alkenylated product as a single atropisomer. The catalytic cycle is completed by the reoxidation of palladium(0) to palladium(II) by the silver salt (Scheme 12).

In continuation of their studies, Colobert and co-workers developed an *atropo*-diastereoselective C–H acetoxylation reaction (Scheme 13a).[48] The use of acetic acid as a co-solvent in the presence of a catalytic amount of $Pd(OAc)_2$ and 2 equivalents of ammonium persulfate as an oxidant permitted selective C–H oxidation to give the corresponding atropo-enriched acetate-substituted biaryls **43**. This acetoxylation reaction is extremely robust, no precautions to avoid air or moisture are required, and the addition of a small amount of water is even beneficial. Under the optimized reaction conditions, a variety of substituted biaryl sulfoxides **42** underwent atroposelective acetoxylation with remarkable efficiency and stereoselectivity. Both electron-donating and electron-withdrawing substituents could be installed at either the 2′-position or the 6-position, and the

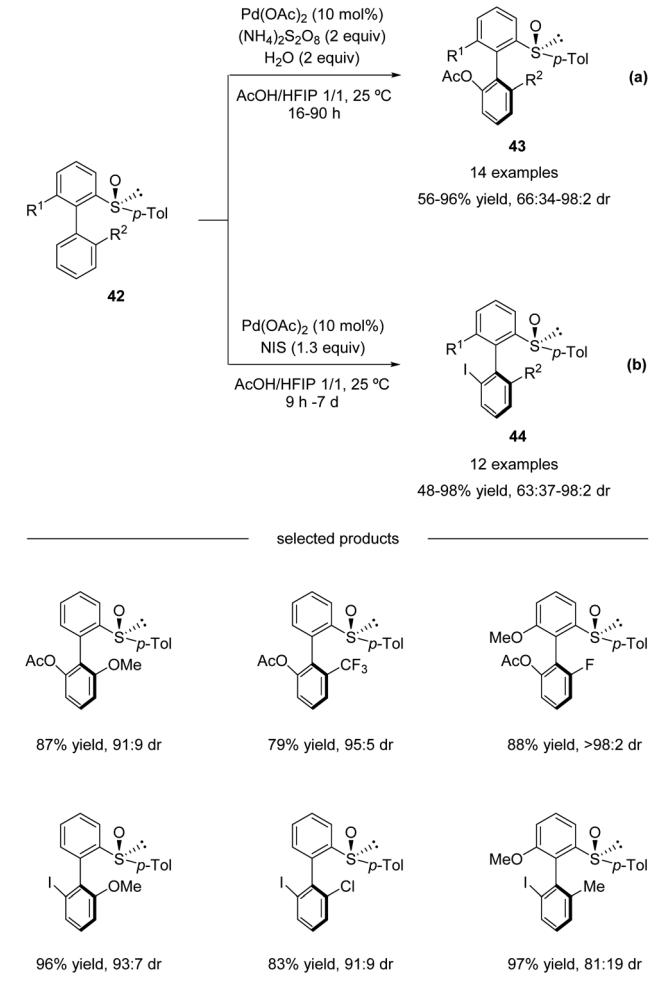

Scheme 13 Pd(II)-catalyzed sulfoxide-directed *atropo*-diastereoselective C–H acetoxylation and halogenation of biphenyls. (a) C–H acetoxylation. (b) C–H iodination.

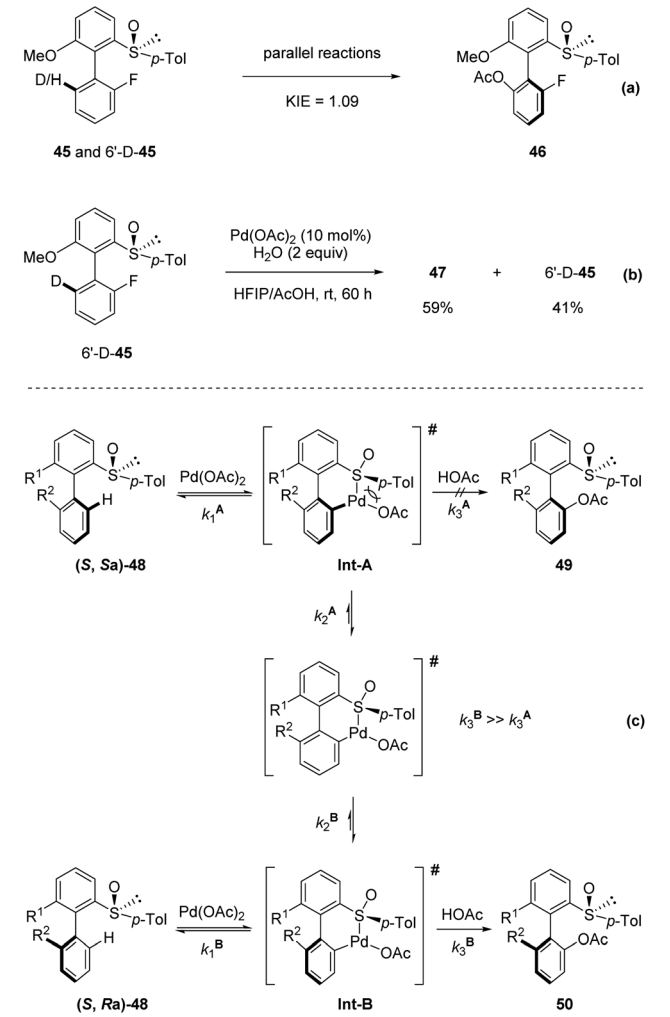

Scheme 14 Mechanistic studies and proposed mechanism. (a) KIE experiment. (b) D/H scrambling experiment. (c) Proposed mechanism.

corresponding C–O coupling products **43** were isolated in 56–96% yields with 66 : 34 to > 98 : 2 diastereoselectivities.

Moreover, this methodology could also be efficiently used for the construction of halogenated *atropo*-pure products **44** (Scheme 13b). A simple replacement of the $(NH_4)_2S_2O_8$ oxidant by *N*-iodosuccinimide (NIS; 1.3 equiv.) led to a complete switch in the reactivity of the catalytic system, which allowed a smooth, mild, and highly diastereoselective C–I coupling reaction.

They undertook several mechanistic studies. First, a kinetic isotope effect of 1.09 was observed through two parallel reactions, verifying that C–H activation was not the rate-determining step (Scheme 14a). Second, when 6′-D-**45** was reacted with $Pd(OAc)_2$ in HFIP/AcOH, a significant D/H scrambling was observed, indicating that the C–H activation step was reversible (Scheme 14b). These results indicate that the overall outcome of this transformation is probably controlled by the kinetics of isomerization of the palladacycle and reductive elimination. They proposed that the steric hindrance around the biaryl axis was high enough to prevent *atropo*-epimerization (rotation around the biaryl axis) of the substrate **48**. Then, the two diastereomers reacted with $Pd(OAc)_2$ rapidly to generate the corresponding *atropo*-stereogenic palladacyclic intermediates **Int-A** and **Int-B**. The formation of such pallada-bridged cyclic species might increase the angle between the two aromatic units, thereby lowering the rotation barrier in this intermediate compared with that in the corresponding substrate, making rotation around the Ar–Ar bond possible. As the steric hindrance of such an intermediate was reduced when palladation occurred on the opposite side of the *p*-tolyl substituent of the sulfoxide moiety, the disfavored palladacycle **Int-A** underwent rapid *atropo*-epimerization to form **Int-B**. In this scenario, the reductive elimination from **Int-A** is unfavored and sufficiently slow to enable isomerization. Finally, reductive elimination from **Int-B** provided the product with high diastereoselectivity (Scheme 14c).

Later in 2018, Wencel-Delord and Colobert developed an elegant *atropo*-diastereoselective arylation reaction, affording terphenyls with two atropisomeric axes (Scheme 15).[49] In this reaction, the sulfoxide moiety served as both the directing group and the chiral auxiliary, allowing the control of double chiral axes with excellent stereoselectivity in a single transformation without any other chiral ligands. Further elaboration of the arylation products generated a series of chiral terphenyl scaffolds, including diphosphine BiaxPhos **57** and S/N-Biax **58**, which was successfully applied in the asymmetric hydrogenation of methyl (*Z*)-α-acetamidocinnamate and asymmetric 1,2-addition of Et_2Zn to benzaldehyde.

Combining D/H scrambling and KIE experiments, they proposed that the first stereogenic axis was established *via* a dynamic kinetic resolution (DKR) process. The diastereomer (*Sa*,*S*)-**59** reacted irreversibly with the NHC–Pd catalyst, whereby the interactions between the *p*-Tol moiety and the NHC ligand

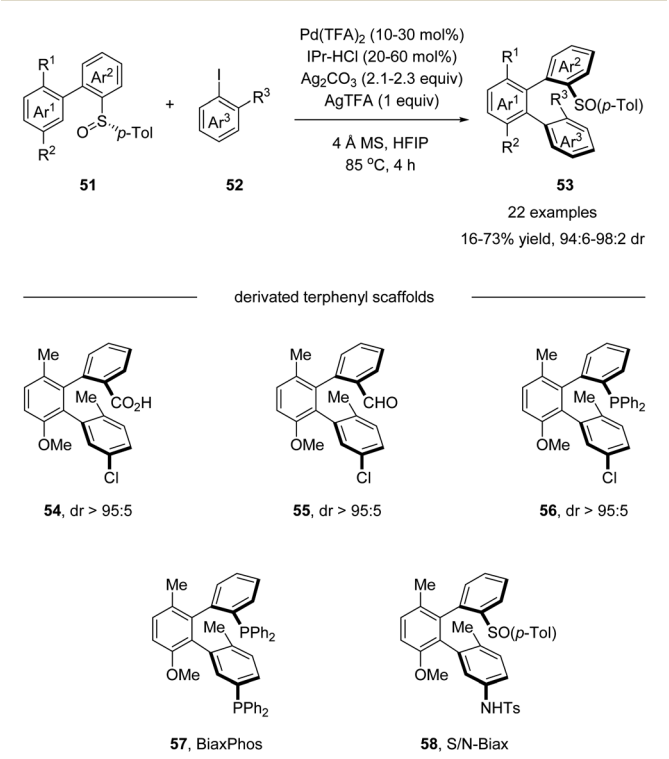

Scheme 15 Pd(II)-catalyzed sulfoxide-directed *atropo*-diastereoselective C–H arylation for the synthesis of terphenyls.

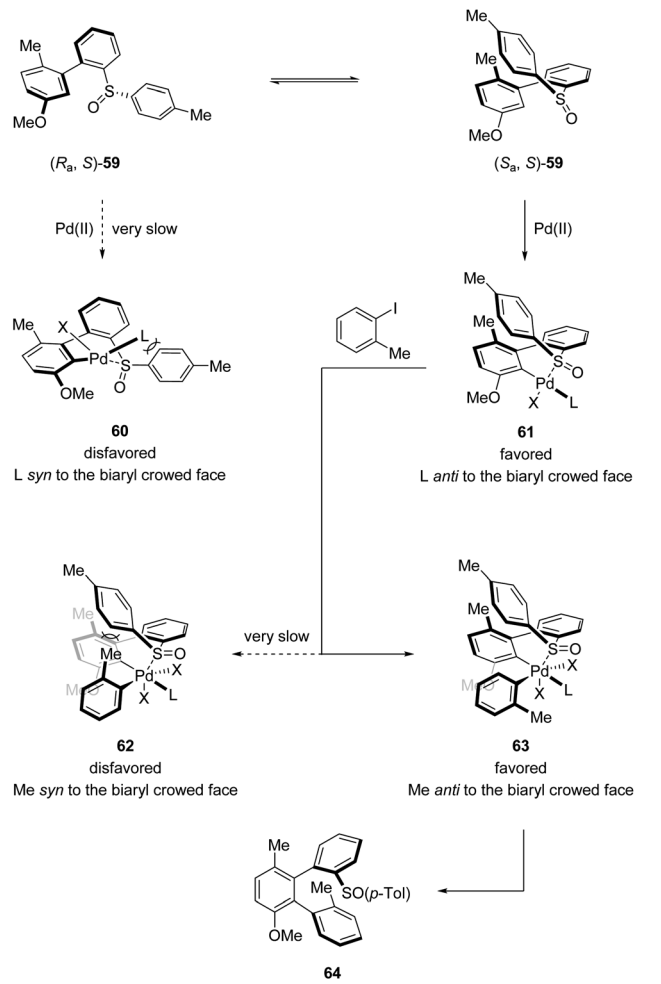

Scheme 16 Possible mechanism for stereoinduction.

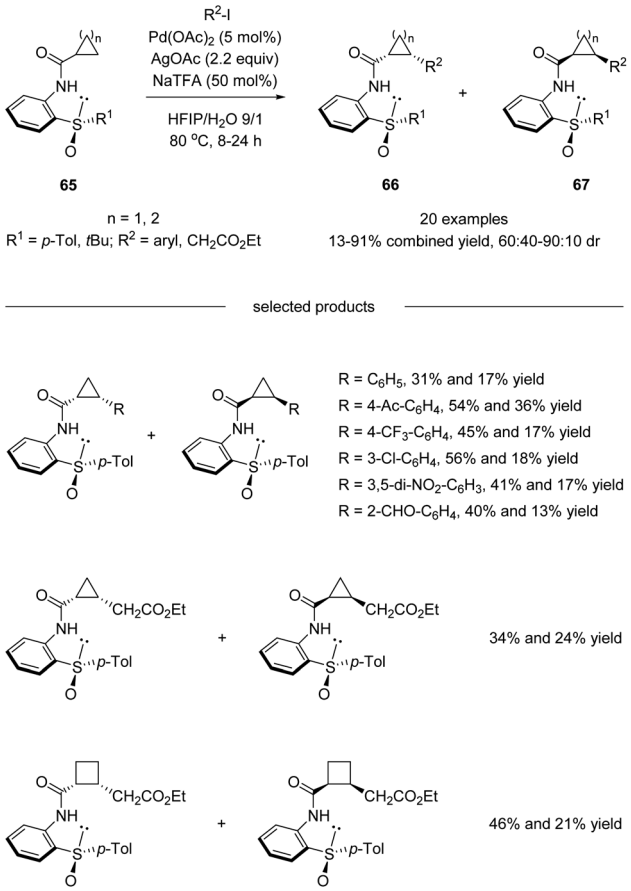

Scheme 17 Chiral APS as a recyclable auxiliary for asymmetric C(sp^3)–H activation.

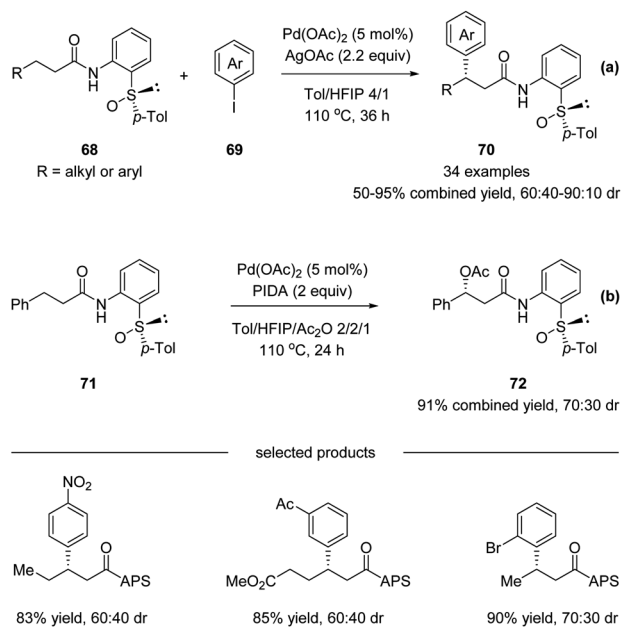

Scheme 18 Stereoselective APS-directed Pd(II)-catalyzed C–H arylation and acetoxylation of aliphatic amides. (a) C–H arylation. (b) C–H acetoxylation.

are minimized. In contrast, the palladation of (*R*a,*S*)-**59** requires the accommodation of the bulky ligand and *p*-Tol moiety in the same plane, enforcing the isomerization of (*R*a,*S*)-**59** to (*S*a,*S*)-**59**, forming the dominant palladacycle **61**. Next, in the induction of the second stereogenic axis, the steric hindrance between the *p*-Tol moiety and the *ortho* substituent of the Ar–I coupling partner is the key element, making **63** the favored oxidative addition intermediate. Finally, reductive elimination from this sterically less congested Pd(IV) intermediate afforded the desired terphenyl product **64** (Scheme 16).

Besides diastereoselective C(sp^2)–H functionalization mentioned above, more challenging asymmetric C(sp^3)–H activation using sulfoxide as the directing chiral auxiliary has also been realized. In 2016, Wencel-Delord, Colobert and co-workers developed a chiral bidentate aniline sulfoxide-based directing group, which allowed a Pd(II)-catalyzed diastereoselective functionalization of the aliphatic C–H bond of cyclopropane and cyclobutane carboxylic acid derivatives (Scheme 17).[50] Both arylation and more challenging alkylation reactions have been investigated, and moderate to good levels of diastereoselectivities could be obtained. It is worth mentioning that the APS (2-(*p*-tolylsulfinyl)aniline) directing group could be cleaved and recovered conveniently after the diastereoselective C(sp^3)–H functionalization without the loss of optical purity.

Later in 2017, Wencel-Delord, Colobert and co-workers reported another application of the APS auxiliary for a Pd(II)-catalyzed diastereoselective C(sp^3)–H arylation of aliphatic amides **68** (Scheme 18a).[51] A wide scope of aryl iodide coupling partners was tolerated for this diastereoselective functionalization of linear aliphatic chains. Moreover, a diastereoselective acetoxylation could also be conducted efficiently, delivering the desired C–O coupling products **72** in high yields yet with moderate dr (Scheme 18b). It is noteworthy that when using a simple amide substrate **73**, a sequential C(sp^3)–H arylation could be performed. One-pot, two-step diarylation of **73** afforded difunctionalized products **75** with two same aryl groups (Scheme 19a) and **78** with two different aryl groups (Scheme 19b).

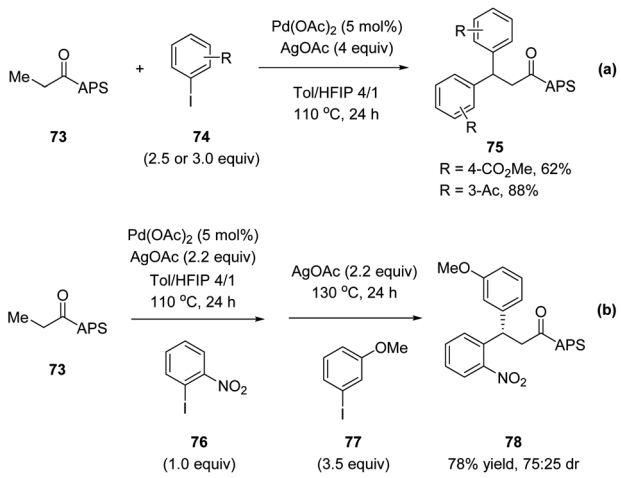

Scheme 19 Stereoselective APS-directed Pd(II)-catalyzed double C–H arylation. (a) Two same aryl groups. (b) Two different aryl groups.

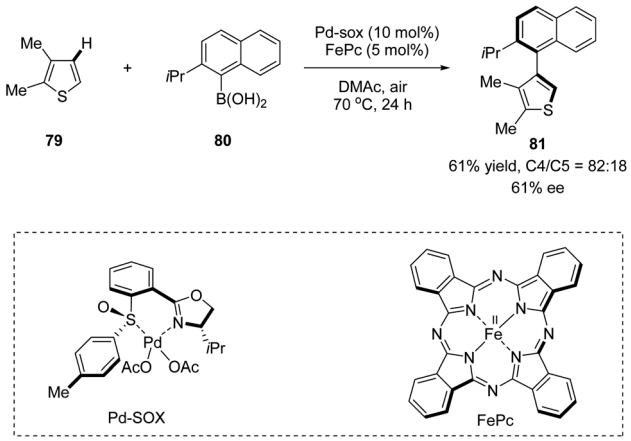

Scheme 20 Sulfoxide–oxazoline ligand enabled atroposelective aerobic oxidative C–H arylation.

3.2 Chiral sulfoxide ligand enabled enantioselective C–H functionalization

In 2013, Yamaguchi, Itami, and co-workers applied a chiral sulfoxide–oxazoline ligand in a Pd(II)/Fe(II) catalyzed C–H arylation reaction (Scheme 20).[52] This is the very first example of the construction of axial chirality using sulfoxide–oxazoline as the chiral ligand. The cross-coupling of 2,3-dimethylthiophene

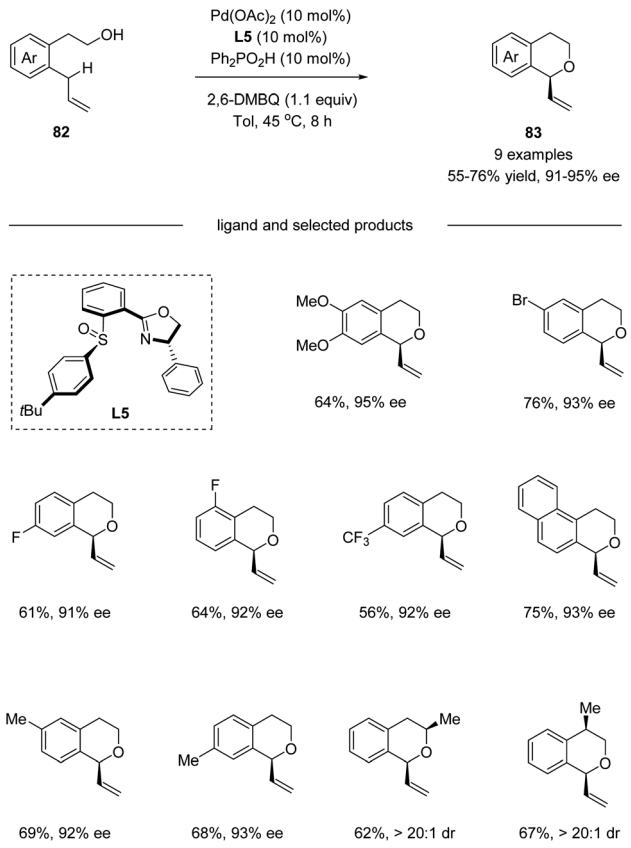

Scheme 21 Pd(II)/chiral sulfoxide catalyzed enantioselective allylic C–H oxidation.

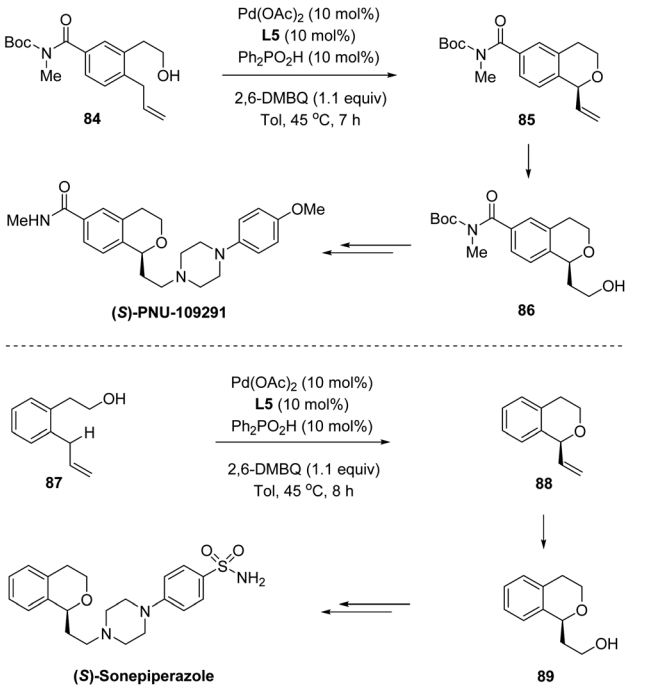

Scheme 22 Vinylisochromans as versatile chiral intermediates.

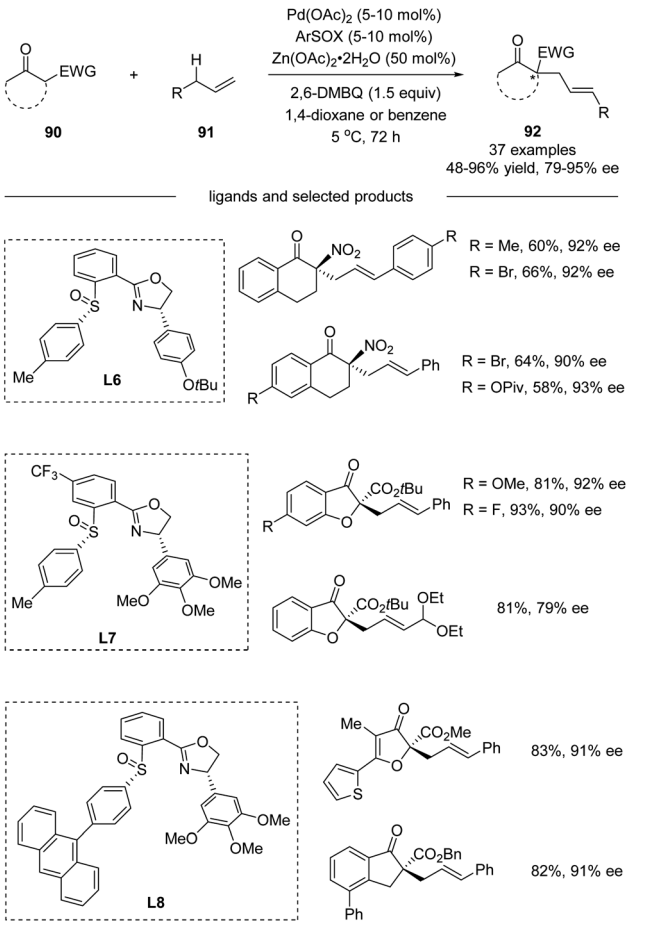

Scheme 23 Asymmetric intermolecular allylic C–H alkylation *via* Pd(II)/*cis*-ArSOX catalysis.

79 with (2-isopropylnaphthalen-1-yl)-boronic acid **80** in the presence of 10 mol% Pd–SOX and 5 mol% FePc as catalysts in dimethylacetamide (DMAc) at 70 °C under air gave the direct C–H arylation product **81** in 61% yield, with 82 : 18 rr and 61% ee.

In 2016, by using chiral sulfoxide–oxazoline **L5** as the ligand, White and co-workers developed a palladium(II)-catalyzed enantioselective intramolecular allylic C–H oxidation of prochiral C–H bonds (Scheme 21).[53] Under optimized conditions, a series of chiral isochromans **83** could be obtained in good yields with excellent enantioselectivities. Taking advantage of this process, bio-active (*S*)-PNU-109291 and (*S*)-sonepiperazole were smoothly synthesized (Scheme 22).

Further in 2018, White and co-workers reported the development of Pd(II)/*cis*-aryl sulfoxide–oxazoline (*cis*-ArSOX) catalysts for asymmetric allylic C–H alkylation of terminal olefins with a variety of synthetically versatile nucleophiles (Scheme 23).[54] The modular, tunable, and oxidatively stable ArSOX scaffold is key to the broad substrate scope and high enantioselectivity (37 examples, 79–95% ee).

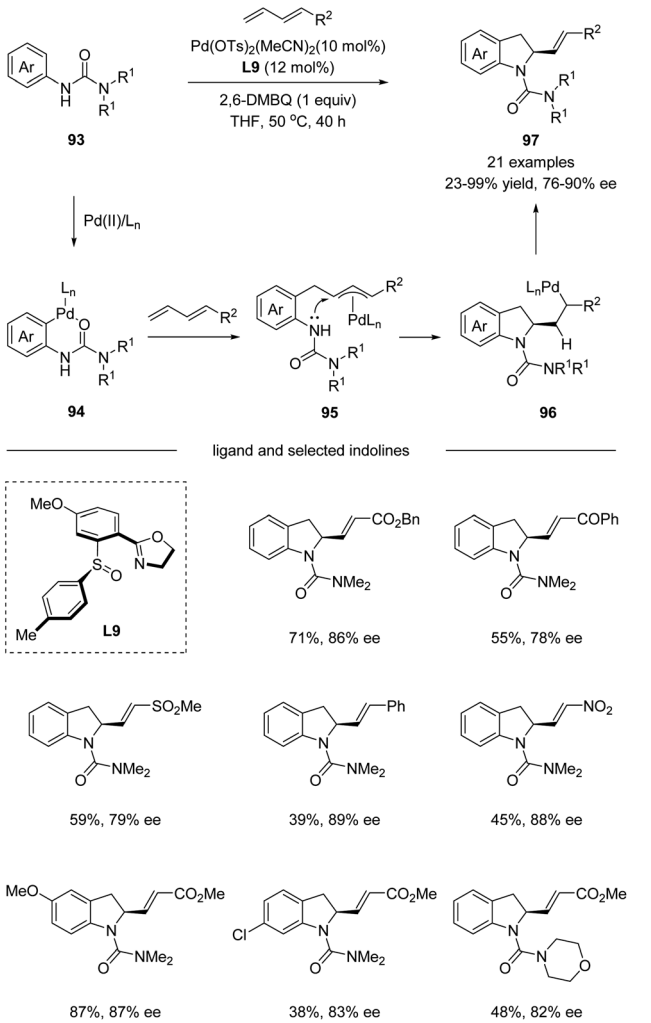

Scheme 24 Pd(II)-catalyzed cascade sp^2 C–H activation/intramolecular asymmetric allylation.

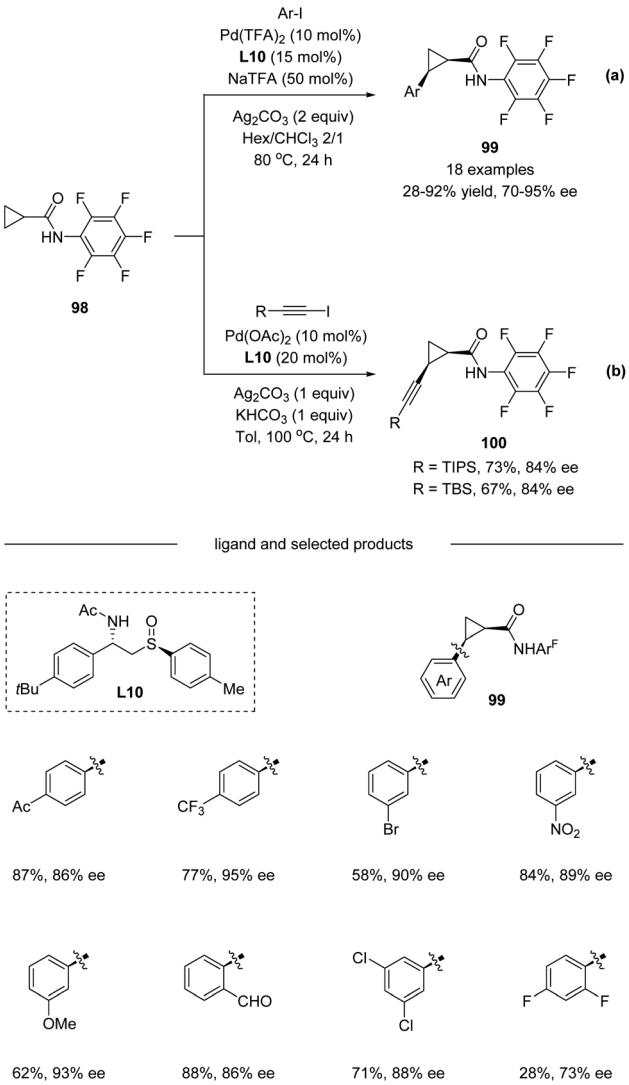

Scheme 25 Pd(II)-catalyzed C(sp^3)–H arylation and alkynylation enable by chiral sulfoxide–amide ligands. (a) C–H arylation. (b) C–H alkynylation.

In 2017, Han and co-workers utilized chiral sulfoxide–oxazoline ligand (SOX) in a palladium-catalyzed cascade sp^2 C–H activation/intramolecular asymmetric allylation reaction (Scheme 24).[55] The process underwent a directing group assisted sp^2 C–H palladation, followed by alkene insertion and asymmetric intramolecular allylation *via* an electrophilic palladation pathway. It is worth mentioning that the chiral sulfoxide–oxazoline ligand **L9** bearing a single chiral center on the sulfur was identified as the optimal ligand for the reaction. A wide range of terminal substituted 1,3-dienes bearing ester, acyl, sulfonyl, and nitro groups reacted smoothly with a series of aryl ureas **93**, affording the corresponding indoline products **97** with excellent *E*/*Z* selectivity and high enantioselectivities.

In 2019, Wencel-Delord, Colobert and co-workers developed a new family of chiral sulfoxide–amide ligands **L10** for a Pd(II)-catalyzed asymmetric C(sp^3)–H arylation of cyclopropanes (Scheme 25a).[56] A variety of Ar–I bearing electron-donating

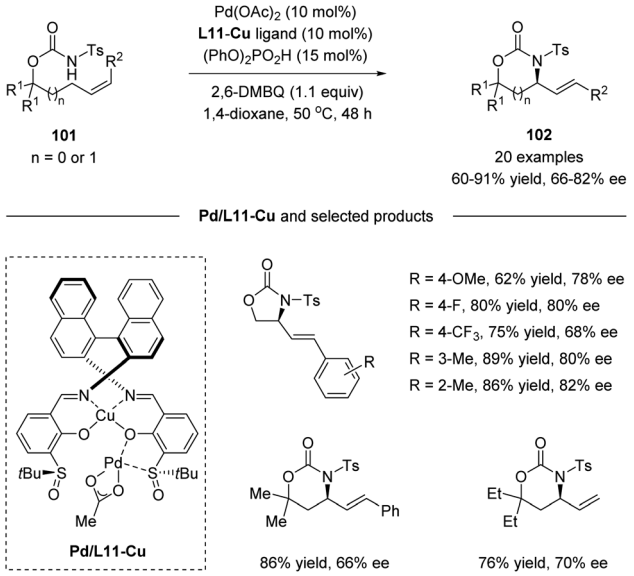

Scheme 26 Cu-containing Schiff base/sulfoxide ligands for a Pd(II)-catalyzed asymmetric allylic C–H amination.

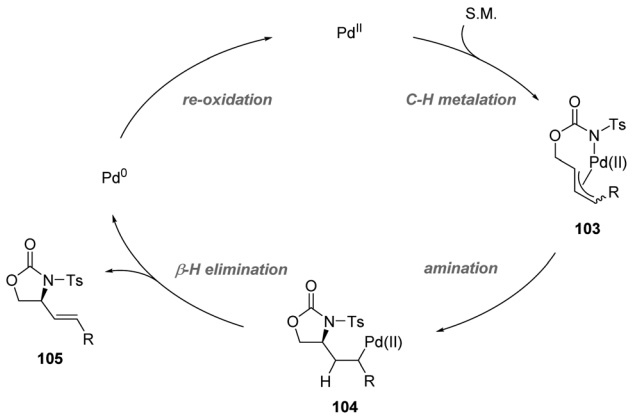

Scheme 27 Possible mechanism.

substituents like OMe and electron-withdrawing substituents such as CF_3, CO_2Me, and Ac were all compatible in the reaction, affording corresponding products **99** with up to 95% ee. Moreover, direct alkynylation could also be performed with an enantioselectivity of up to 84% ee. Nevertheless, the substrate scope for alkynylation is limited in TIPS and TBS protected alkynyl iodide (Scheme 25b).

Recently, Yoshino, Matsunaga and co-workers demonstrated the synthetic utility of Cu-containing Schiff base/sulfoxide ligands for a Pd(II)-catalyzed asymmetric allylic C–H amination reaction (Scheme 26).[57] The combination of the Schiff base-Cu(II)/sulfoxide with $Pd(OAc)_2$ provided intramolecular C–H amination products with up to 82% ee. DFT calculations suggested that the chelation of the palladium complex by the sulfoxide and phenoxide lone pair is energetically favored, delivering the best outcome of enantioselectivity. Both internal and terminal alkenes were applicable in the transformation. The reaction is proposed to start with an allylic C–H activation, generating a Pd(II)-allyl intermediate **103**. Then asymmetric amination followed by β-hydride elimination afforded the chiral product and Pd(0). Finally, the re-generation of Pd(II) finished the catalytic cycle (Scheme 27).

4. Conclusions

The past decade has witnessed the rapid development of the field of enantioselective C–H functionalization, and this transformation has gradually become a powerful tool for the synthesis of valuable chiral molecules. In particular, the use of sulfur-based directing groups has delivered a variety of new stereoselective C–H transformations *via* various activation modes, which have been incorporated into synthetic routes to many chiral organosulfur compounds. This perspective summarizes recent progress in the generation and utilization of sulfur stereogenic centers in asymmetric C–H transformations, including the construction of sulfur stereogenic centers of sulfoxide and sulfoximines *via* enantioselective C–H functionalization based on desymmetrization and (parallel) kinetic resolution strategies and chiral sulfoxide directing group or chiral sulfoxide ligand enabled stereoselective C–H functionalization.

Currently, the generation of sulfur stereocenters *via* C–H functionalization relies on desymmetrization and kinetic resolution pathways. New strategies are in high demand. The utilization of chiral sulfoxides as directing groups and ligands for stereoselective C–H functionalization has witnessed enormous growth, which allow the synthesis of optically active products with high yields and enantioselectivities. However, the scope of reactions using such directing groups and ligands remains limited, and the development of new types of ligands and reactions will be the topic of this area in the future. We believe that accessing and utilizing sulfur stereocenters *via* asymmetric C–H functionalization represents a continuously expanding field with exciting chances to develop new transformations with broad application potential.

Author contributions

C. H. and W. L. convinced the topic and assembled all the sections. W. L., J. K. and C. H. wrote and edited the manuscript.

Conflicts of interest

There are no conflicts to declare.

Acknowledgements

We are grateful for financial support from the start-up fund from the Southern University of Science and Technology, Shenzhen Science and Technology Innovation Committee (JCYJ20190809142809370), and Guangdong Provincial Key Laboratory of Catalysis (No. 2020B121201002).

Notes and references

1 *Handbook of C–H Transformations: Applications in Organic Synthesis*, ed. G. Dyker, vol. 2, 2005.
2 K. Godula and D. Sames, *Science*, 2006, **312**, 67–72.
3 O. Daugulis, H.-Q. Do and D. Shabashov, *Acc. Chem. Res.*, 2009, **42**, 1074–1086.
4 D. A. Colby, R. G. Bergman and J. A. Ellman, *Chem. Rev.*, 2010, **110**, 624–655.
5 T. W. Lyons and M. S. Sanford, *Chem. Rev.*, 2010, **110**, 1147–1169.
6 I. A. I. Mkhalid, J. H. Barnard, T. B. Marder, J. M. Murphy and J. F. Hartwig, *Chem. Rev.*, 2010, **110**, 890–931.
7 Y. Park, Y. Kim and S. Chang, *Chem. Rev.*, 2017, **117**, 9247–9301.
8 C. Zheng and S.-L. You, *RSC Adv.*, 2014, **4**, 6173–6214.
9 C. G. Newton, S.-G. Wang, C. C. Oliveira and N. Cramer, *Chem. Rev.*, 2017, **117**, 8908–8976.
10 T. G. Saint-Denis, R.-Y. Zhu, G. Chen, Q.-F. Wu and J.-Q. Yu, *Science*, 2018, **359**, 759.
11 J. Diesel and N. Cramer, *ACS Catal.*, 2019, **9**, 9164–9177.
12 J. Loup, U. Dhawa, F. Pesciaioli, J. Wencel-Delord and L. Ackermann, *Angew. Chem., Int. Ed.*, 2019, **58**, 12803–12818.
13 R. Bentley, *Chem. Soc. Rev.*, 2005, **34**, 609–624.
14 P. Lindberg, A. Braendstroem, B. Wallmark, H. Mattsson, L. Rikner and K. J. Hoffmann, *Med. Res. Rev.*, 1990, **10**, 1–54.
15 I. Agranat and H. Caner, *Drug Discovery Today*, 1999, **4**, 313–321.
16 A. R. Maguire, S. Papot, A. Ford, S. Touhey, R. O'Connor and M. Clynes, *Synlett*, 2001, **1**, 41–44.
17 A. Osorio-Lozada, T. Prisinzano and H. F. Olivo, *Tetrahedron: Asymmetry*, 2004, **15**, 3811–3815.
18 J. Legros, J. R. Dehli and C. Bolm, *Adv. Synth. Catal.*, 2005, **347**, 19–31.
19 Q. Tang, X. Yin, R. R. Kuchukulla, Q. Zeng and R. R. Kuchukulla, *Chem. Rec.*, 2021, **21**, 893–905.
20 D. Kaiser, I. Klose, R. Oost, J. Neuhaus and N. Maulide, *Chem. Rev.*, 2019, **119**, 8701–8780.
21 J. Lou, Q. Wang, P. Wu, H. Wang, Y.-G. Zhou and Z. Yu, *Chem. Soc. Rev.*, 2020, **49**, 4307–4359.
22 N. Sundaravelu, S. Sangeetha and G. Sekar, *Org. Biomol. Chem.*, 2021, **19**, 1459–1482.
23 M. Carmen Carreno, G. Hernandez-Torres, M. Ribagorda and A. Urbano, *Chem. Commun.*, 2009, **41**, 6129–6144.
24 G. Sipos, E. E. Drinkel and R. Dorta, *Chem. Soc. Rev.*, 2015, **44**, 3834–3860.
25 B. M. Trost and M. Rao, *Angew. Chem., Int. Ed.*, 2015, **54**, 5026–5043.
26 S. Otocka, M. Kwiatkowska, L. Madalinska and P. Kielbasinski, *Chem. Rev.*, 2017, **117**, 4147–4181.
27 T. Jia, M. Wang and J. Liao, *Top. Curr. Chem.*, 2019, **377**, 1–29.
28 I. Fernandez and N. Khiar, *Chem. Rev.*, 2003, **103**, 3651–3705.
29 E. Wojaczynska and J. Wojaczynski, *Chem. Rev.*, 2010, **110**, 4303–4356.
30 A. P. Pulis and D. J. Procter, *Angew. Chem., Int. Ed.*, 2016, **55**, 9842–9860.
31 C. Sambiagio, D. Schonbauer, R. Blieck, T. Dao-Huy, G. Pototschnig, P. Schaaf, T. Wiesinger, M. F. Zia, J. Wencel-Delord, T. Besset, B. U. W. Maes and M. Schnurch, *Chem. Soc. Rev.*, 2018, **47**, 6603–6743.
32 K.-X. Tang, C.-M. Wang, T.-H. Gao, L. Chen, L. Fan and L.-P. Sun, *Adv. Synth. Catal.*, 2019, **361**, 26–38.
33 Y.-C. Zhu, Y. Li, B.-C. Zhang, F.-X. Zhang, Y.-N. Yang and X.-S. Wang, *Angew. Chem., Int. Ed.*, 2018, **57**, 5129–5133.
34 W. Liu, W. Yang, J. Zhu, Y. Guo, N. Wang, J. Ke, P. Yu and C. He, *ACS Catal.*, 2020, **10**, 7207–7215.
35 B. Shen, B. Wan and X. Li, *Angew. Chem., Int. Ed.*, 2018, **57**, 15534–15538.
36 Y. Sun and N. Cramer, *Angew. Chem., Int. Ed.*, 2018, **57**, 15539–15543.
37 M. Brauns and N. Cramer, *Angew. Chem., Int. Ed.*, 2019, **58**, 8902–8906.
38 D. P. Walker, M. P. Zawistoski, M. A. McGlynn, J.-C. Li, D. W. Kung, P. C. Bonnette, A. Baumann, L. Buckbinder, J. A. Houser, J. Boer, A. Mistry, S. Han, L. Xing and A. Guzman-Perez, *Bioorg. Med. Chem. Lett.*, 2009, **19**, 3253–3258.
39 M. Frings, C. Bolm, A. Blum and C. Gnamm, *Eur. J. Med. Chem.*, 2017, **126**, 225–245.
40 T. Zhou, P.-F. Qian, J.-Y. Li, Y.-B. Zhou, H.-C. Li, H.-Y. Chen and B.-F. Shi, *J. Am. Chem. Soc.*, 2021, **143**, 6810–6816.
41 S. Ogawa and N. Furukawa, *J. Org. Chem.*, 1991, **56**, 5723–5726.
42 C. Quesnelle, T. Iihama, T. Aubert, H. Perrier and V. Snieckus, *Tetrahedron Lett.*, 1992, **33**, 2625–2628.
43 B. Ferber and H. B. Kagan, *Adv. Synth. Catal.*, 2007, **349**, 493–507.
44 J. L. G. Ruano and A. M. M. Castro, *Heteroat. Chem.*, 2007, **18**, 537–548.
45 *Organosulfur Chemistry in Asymmetric Synthesis*, ed. T. Toru and C. Bolm, Wiley-VCH Verlag GmbH & Co. KGaA, 2008.
46 T. Wesch, F. R. Leroux and F. Colobert, *Adv. Synth. Catal.*, 2013, **355**, 2139–2144.
47 Q. Dherbassy, G. Schwertz, M. Chesse, C. K. Hazra, J. Wencel-Delord and F. Colobert, *Chem.–Eur. J.*, 2016, **22**, 1735–1743.
48 C. K. Hazra, Q. Dherbassy, J. Wencel-Delord and F. Colobert, *Angew. Chem., Int. Ed.*, 2014, **53**, 13871–13875.
49 Q. Dherbassy, J.-P. Djukic, J. Wencel-Delord and F. Colobert, *Angew. Chem., Int. Ed.*, 2018, **57**, 4668–4672.
50 S. Jerhaoui, F. Chahdoura, C. Rose, J.-P. Djukic, J. Wencel-Delord and F. Colobert, *Chem.–Eur. J.*, 2016, **22**, 17397–17406.
51 S. Jerhaoui, J.-P. Djukic, J. Wencel-Delord and F. Colobert, *Chem.–Eur. J.*, 2017, **23**, 15594–15600.
52 K. Yamaguchi, H. Kondo, J. Yamaguchi and K. Itami, *Chem. Sci.*, 2013, **4**, 3753–3757.
53 S. E. Ammann, W. Liu and M. C. White, *Angew. Chem., Int. Ed.*, 2016, **55**, 9571–9575.
54 W. Liu, S. Z. Ali, S. E. Ammann and M. C. White, *J. Am. Chem. Soc.*, 2018, **140**, 10658–10662.
55 S.-S. Chen, M.-S. Wu and Z.-Y. Han, *Angew. Chem., Int. Ed.*, 2017, **56**, 6641–6645.
56 S. Jerhaoui, J.-P. Djukic, J. Wencel-Delord and F. Colobert, *ACS Catal.*, 2019, **9**, 2532–2542.
57 Y. Bunno, Y. Tsukimawashi, M. Kojima, T. Yoshino and S. Matsunaga, *ACS Catal.*, 2021, **11**, 2663–2668.